0026-895X/98/061124-08$3.00/0

MOLECULAR PHARMACOLOGY, **54:**1124–1131 (1998).

Four Pharmacologically Distinct Subtypes of $\alpha4\beta2$ Nicotinic Acetylcholine Receptor Expressed in *Xenopus laevis* Oocytes

RUUD ZWART and HENK P. M. VIJVERBERG

Research Institute of Toxicology, Utrecht University, Utrecht, The Netherlands

Received May 18, 1998; Accepted September 14, 1998

This paper is available online at http://www.molpharm.org

ABSTRACT

Nicotinic receptors generally are presumed to consist of two α and three non-α subunits. We varied the relative levels of expression of the neuronal nicotinic $\alpha4$ and $\beta2$ receptor subunits in *Xenopus laevis* oocytes by nuclear injection of cDNAs coding for these subunits in α:β ratios of 9:1, 1:1, and 1:9. The sensitivities of the receptors to acetylcholine and *d*-tubocurarine were investigated in voltage-clamp experiments. For receptors expressed at the 9:1 and 1:1 α:β ratios, the EC_{50} value of acetylcholine is ~60 μM. For the majority of the receptors expressed at the 1:9 α:β ratio, the sensitivity to acetylcholine is enhanced 30-fold. No evidence for more than one type of acetylcholine binding site in a single receptor is obtained. The sensitivity to *d*-tubocurarine decreases with decreasing α:β ratio. IC_{50} values of *d*-tubocurarine are 0.2, 0.5, and 2 μM for the 9:1, 1:1, and 1:9 α:β ratios, respectively. At the 1:9 α:β ratio, additional receptors with an IC_{50} value of 163 μM *d*-tubocurarine are expressed. At least two components with distinct sensitivities to *d*-tubocurarine are required to account for the shift in IC_{50}. The combined agonist and antagonist effects reveal four distinct subtypes of $\alpha4\beta2$ nicotinic receptors. The results imply that the subunit stoichiometry of heteromeric $\alpha4\beta2$ acetylcholine receptors is not restricted to 2α:3β.

Neuronal nAChRs are ligand-gated ion channels present throughout the central and peripheral nervous systems. Multiple neuronal nAChR subunits ($\alpha2$–9 and $\beta2$–4) have been identified. These subunits combine in various compositions to form pentameric receptors with different functional and pharmacological characteristics (reviewed in McGehee and Role, 1995).

The $\alpha4$ and $\beta2$ nAChR subunits are expressed abundantly in brain (Wada *et al*., 1989), and the most common nAChR in the brain is composed of these two subunits (Whiting *et al*., 1990; Flores *et al*., 1992). The subunit stoichiometry of $\alpha4\beta2$ nAChRs expressed in *Xenopus laevis* oocytes has been deduced to be $\alpha4$:$\beta2$ = 2:3 (Anand *et al*., 1991; Cooper *et al*., 1991), and the subunits are assumed to be arranged around the central ion channel pore in the order $\beta\alpha\beta\alpha\beta$ (Anand *et al*., 1991). Patch-clamp recording from oocytes expressing pairs of α and β nAChR subunits revealed ACh-gated single channels with distinct conductances (Papke *et al*., 1989; Papke and Heinemann, 1991; Charnet *et al*., 1992; Kuryatov *et al*., 1997). The frequency of occurrence of the different single-channel conductance states depends on the α:β ratio of the mRNA mixture injected into the oocyte, indicating that receptors with different subunit stoichiometry are expressed (Papke *et al*., 1989).

The agonist binding sites of heteropentameric neuronal nAChRs generally are supposed to be located at the two $\alpha\beta$ subunit interfaces (reviewed in Bertrand and Changeux, 1995). Functional nAChRs with distinct subunit stoichiometries might differ with respect to the number and properties of agonist binding sites. We investigated the functional properties of the agonist binding sites in *X. laevis* oocytes expressing different levels of $\alpha4$ and $\beta2$ nAChR subunits. The results on concentration-dependent effects of the agonist ACh and of d-TC, a competitive antagonist of $\alpha4\beta2$ nAChRs (Bertrand *et al*., 1990), demonstrate four distinct subtypes of $\alpha4\beta2$ nAChRs.

Experimental Procedures

Materials. *X. laevis* were bred and kept in the Hubrecht Laboratory (Utrecht, The Netherlands) or were bought from Nasco (Fort Atkinson, WI) and kept in our own laboratory. Neomycin was obtained from Sigma Chemical (St. Louis, MO). d-TC was from Fluka (Buchs, Switzerland). All other materials used came from sources identical to those described previously (Zwart and Vijverberg, 1997).

Receptor expression. Oocytes were prepared, injected, and incubated in Barth's solution containing 5 mg/liter of neomycin at 19° for 3–7 days as described previously (Zwart *et al*., 1995; Zwart and Vijverberg, 1997). Plasmids coding for $\alpha4$ and $\beta2$ subunits of neuronal nAChRs were dissolved in distilled water at the approximately equal concentrations of 152 ± 15 and 136 ± 12 μg/ml (mean ± standard deviation of triplicate spectrophotometric determinations),

This work was financially supported by Netherlands Organization for Scientific Research (NWO) Grant 903–42-011.

ABBREVIATIONS: nAChR, nicotinic acetylcholine receptor; ACh, acetylcholine; ANOVA, analysis of variance; d-TC, *d*-tubocurarine; HEPES, 4-(2-hydroxyethyl)-1-piperazineethanesulfonic acid.

respectively. Unless noted otherwise, mixtures of these solutions at 1:9, 1:1, and 9:1 ratios were coinjected at 18.4 nl/oocyte.

Electrophysiology and data analysis. Oocytes were placed in a silicon rubber tube (diameter, 3 mm), penetrated by two microelectrodes, and voltage clamped at −80 mV. ACh and d-TC, dissolved in external solution, were applied by perfusion of the tube at a rate of ~20 ml/min. The external saline contained 115 mM NaCl, 2.5 mM KCl, 1 mM $CaCl_2$, and 10 mM HEPES, pH 7.2, with NaOH. Voltage-clamp equipment, experimental protocols, and data acquisition were exactly as described previously (Zwart and Vijverberg, 1997). All amplitudes of ACh-induced ion currents were normalized to the amplitude of alternately evoked control responses to a near-maximum effective concentration of ACh to adjust for small variations in response amplitude over time. Data are expressed as mean ± standard deviation of number of oocytes. ANOVA was performed using Microsoft Excel. Results were compared using a two-tailed Student's *t* test. Concentration-effect curves were fitted, using Jandel SigmaPlot software, to data obtained in separate experiments, and mean ± standard deviation values of estimated parameters were calculated for three oocytes. Curves drawn in the figures were generated using the mean values of the estimated parameters. Agonist data were fitted according to the equations $i/i_{max} = E_{max}/[1 + (EC_{50}/[ACh])^{nH}]$ and $i/i_{max} = E_{maxa}/(1 + EC_{50a}/[ACh]) + E_{maxb}/(1 + EC_{50b}/[ACh])$ for one- and two-component activation curves, respectively. Antagonist data were fitted according to the equations: $i/i_{max} = 1/[1 + ([dTC]/IC_{50})^{nH}]$ and $i/i_{max} = E_m/[1 + ([dTC]/IC_{50a})^{nHa}) + (1 - E_m)/[1 + ([dTC]/IC_{50b})^{nHb}]$ for one- and two-component inhibition curves, respectively. In these equations, [ACh] and [dTC] are the concentrations of ACh and d-TC, respectively; n_H is the Hill coefficient; and i/i_{max} is the normalized current amplitude. Goodness-of-fit was judged by analysis of the residuals (run test).

Results

Effects of α4:β2 ratio on ion current amplitude. Superfusion of voltage-clamped oocytes, expressing α4β2 nAChRs after the injection of α4 and β2 subunit cDNAs in the α:β ratios 1:9, 1:1, and 9:1, with 300 μM ACh results in ligand-gated ion currents. The effect of subunit ratio on response amplitude was investigated in the same batch of oocytes because expression levels vary between batches. The amplitude of the inward current induced by the near-maximal effective concentration of 300 μM ACh at the holding potential of −80 mV depends on the α4:β2 subunit cDNA ratio injected into the oocytes (Fig. 1). The largest inward currents are observed in oocytes injected with α4 and β2 subunit cDNAs in the 1:1 ratio. At both the 1:9 and 9:1 α:β ratios, amplitudes of inward currents evoked by 300 μM ACh are reduced significantly (*t* test; $p < 0.001$). Some oocytes (9 of 54) that did not respond to ACh at all, most likely because the cDNA was not properly injected into the nucleus, were excluded from the analysis. The results show that, after injection of the α4 and β2 subunit cDNAs in extreme ratios, while maintaining the total cDNA injected approximately constant, inward current amplitudes are reduced. This indicates that after injection of cDNAs in the α:β ratios of 1:9 and 9:1, response amplitude is limited by the availability of α and β subunits, respectively. After injection of the same total amounts of either cDNA encoding the α4 subunit only or cDNA encoding the β2 subunit only, oocytes did not respond to 300 μM ACh (results not shown). This demonstrates that α4 and β2 subunits do not form functional homopentameric nAChRs. The absence of ACh-induced inward current also shows that α4 and β2 do not form functional heteromeric nAChRs with native nAChR subunits that possibly are present in *X. laevis* oocytes (Buller and White, 1990).

Effects of α4:β2 ratio on the agonist concentration-effect curve. Agonist concentration-effect curves were obtained from oocytes expressing α4β2 nAChRs after the injection of subunit cDNAs in the α:β ratios of 1:9, 1:1, and 9:1. Examples of ACh-induced ion currents are shown in Fig. 2A for the different subunit cDNA ratios tested.

From Fig. 2A, it is apparent that inward currents evoked by high concentrations of ACh show an acceleration of inward current decay. In addition, a "tail" inward current is observed on removal of the agonist. These effects are commonly attributed to the onset and reversal of ion channel block by high concentrations of ACh (Colquhoun and Ogden, 1988; Oortgiesen and Vijverberg, 1989). For the different α:β ratios, inward current decay in the absence of overt ion channel block (i.e., for responses evoked by superfusion with 300 μM ACh) was quantified by dividing the inward current at the end of ACh application (t = 10 sec) by the peak inward current. The inward current decayed to 61 ± 16% (5 oocytes) of the peak value for the 1:1 α:β ratio, to 51 ± 11% (7 oocytes) for the 9:1 α:β ratio, and to 82 ± 4% (14 oocytes) for the 1:9 α:β ratio. The degree of inward current decay at the 1:9 ratio differs significantly from that at the 1:1 and 9:1 α:β ratios (*t* test; $p < 0.05$).

For each of the α:β subunit cDNA ratios investigated, the amplitudes of peak inward current evoked by superfusion of 0.1 μM to 10 mM ACh were normalized to those of 1 mM ACh-induced inward currents in three oocytes. Two-way ANOVA of the results obtained with ACh at concentrations of ≤1 mM showed that the data for the 1:1 and 9:1 α:β ratios cannot be distinguished statistically ($F_{1,28} = 0.1441$, $p = 0.71$) and that both sets of data differ statistically from the data obtained for the 1:9 ratio ($p < 0.001$). Concentration-effect curves of ACh were fitted for each α:β ratio. The data of the 1:1 and 9:1 α:β ratios are closely approximated by one-component sigmoidal curves (Fig. 2B). In all cases, data measured at the higher ACh concentrations, which induce ion channel block, were excluded from the curve-fitting procedure. For the 1:9 α:β ratio, the concentration-effect curve

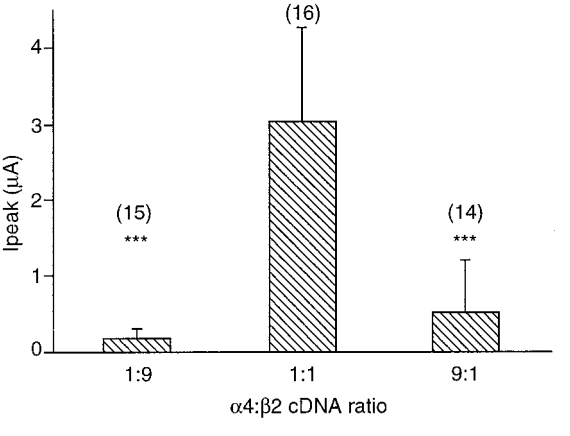

Fig. 1. Peak inward current amplitudes evoked by superfusion with 300 μM ACh in *X. laevis* oocytes expressing α4β2 nAChRs. Oocytes from a single batch were injected with approximately equal amounts of cDNAs encoding α4 and β2 nAChR subunits in the ratios indicated. *Bars*, mean ± standard deviation values of peak amplitudes from the number of oocytes indicated (*between brackets*). Peak amplitudes obtained for the 1:9 and 9:1 α:β ratios are significantly reduced compared with those obtained for the 1:1 α:β ratio (*t* test; $p < 0.001$).

shows a striking shift toward lower agonist concentrations, and the slope of the data is markedly reduced. Together with the inflection point in the data observed between 10 and 100 μM ACh (Fig. 2B), this suggests the presence of two components with distinct sensitivities to the agonist. A one-component concentration-effect curve did not fit the data adequately as indicated by analysis of the residuals (run test; $p < 0.05$). The data obtained for concentrations of <1 mM ACh could be fitted by a two-component concentration-effect curve only with fixed values of the slope factors. EC_{50} values of 1.74 and 144 μM ACh and E_{max} values of 85% and 43%, respectively, were obtained when the slope factors were set to 1. Due to the small number of data available for curve fitting at high agonist concentrations, reliable estimates for the less-sensitive component cannot be obtained. A one-component concentration-effect curve fitted to the data obtained with ACh at concentrations of ≤30 μM yielded EC_{50}, n_H, and E_{max} values of 1.84 μM ACh, 1.05, and 89.3%, respectively (Table 1). The two concentration-effect curves both seem to fit the more-sensitive component accurately (Fig. 2B). The large E_{max} value of the more-sensitive component of the concentration-effect curve indicates that the majority of nAChRs expressed at the 1:9 α:β cDNA ratio are highly sensitive to ACh. Oocytes injected with cDNAs encoding α3 and β2, or α4 and β4, in a 1:9 α:β ratio did not show enhanced sensitivity to ACh compared with oocytes injected with these subunit cDNAs in a 1:1 α:β ratio (not shown).

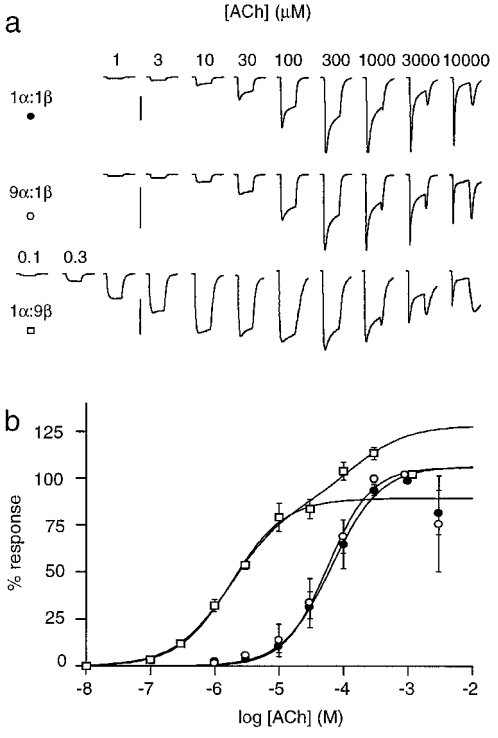

Fig. 2. Concentration-dependent effects of ACh on α4β2 nAChRs expressed in *X. laevis* oocytes after injection of cDNAs in the α:β ratios indicated. a, Inward currents evoked by 10-sec periods of superfusion with external saline containing ACh at the concentrations indicated for three oocytes at the 1:1 (●), 9:1 (○), and 1:9 (□) α:β ratios. *Calibration bars*, 4.5 μA (1:1) and 350 nA (9:1 and 1:9). b, Dependence of inward current amplitude, normalized to the amplitude of control responses induced by 1 mM ACh, on the concentration of ACh. Values are mean ± standard deviation obtained from three oocytes. The data obtained for the 1:1 and 9:1 α:β ratios were fitted adequately by one-component concentration-effect curves (*drawn lines*). Data obtained at concentrations of >300 μM ACh, which induced ion channel block, are not included in the fit. The data obtained for the 1:9 α:β ratio could not be fitted by a one-component concentration-effect curve. The two-component curve drawn was fitted to all data obtained at concentrations of ≤300 μM ACh with slope factors set to 1. The concentration-effect curve describing the component more sensitive to ACh, fitted separately to the data obtained at ≤30 μM ACh, is also drawn. The estimated parameters of the fitted curves are presented in Table 1.

From the ANOVA of the data and from the EC_{50} values estimated from the concentration-effect curves (Table 1), it is concluded that depending on the ratio of α4 and β2 subunit cDNAs injected, two distinct types of functional nAChRs are expressed in oocytes with ~30-fold difference in sensitivity to ACh.

Effects of α4:β2 ratio on the antagonist concentration-effect curve. Concentration-effect curves for the competitive nAChR antagonist d-TC also were obtained from oocytes expressing α4β2 nAChRs after the injection of subunit cDNAs in the α:β ratios of 1:9, 1:1, and 9:1. Examples of ion currents evoked by superfusion of 300 μM ACh in the absence and the presence of various concentrations of d-TC are shown in Fig. 3A for the different subunit cDNA ratios tested. d-TC was superfused ≥4 min before an ACh-induced current was recorded in the presence of d-TC. For three oocytes of each α:β subunit cDNA ratio tested, peak inward current amplitudes were normalized to those of control inward currents evoked by 300 μM ACh in the same oocyte. The normalized data are plotted against d-TC concentration in Fig. 3A. ANOVA of the inhibitory effects of d-TC showed that the data for the different subunit cDNA ratios all are statistically different at the $p < 0.001$ level. For the 9:1 and 1:1 α:β subunit cDNA ratios, data could be fitted by a one-component concentration-effect curve. However, for the 1:9 ratio, the concentration dependence of inhibition by d-TC seemed to be biphasic, and fit was significantly improved by fitting a sum of two concentration-effect curves to the data (Fig. 3A). Estimated values of the parameters of the fitted concentration-effect curves are presented in Table 2. The inhibitory effects of d-TC on α4β2 nAChRs at the 1:1 α:β ratio also were investigated at a holding potential of −40 mV (result not shown). The IC_{50} value for d-TC of 0.91 ± 0.48 μM (three oocytes) at −40 mV could not be distinguished from that obtained at the holding potential of −80 mV. Thus, it seems that voltage-dependent ion channel block, observed previously for muscle-type nAChRs at high concentrations of d-TC (Colquhoun *et al.*, 1979), does not strongly contribute to the inhibitory effects of d-TC observed at concentrations of ≤10 μM.

TABLE 1

Effects of ACh on α4β2 nAChRs expressed in *Xenopus* oocytes injected with cDNAs encoding α and β subunits in the ratios indicated

For each experimental condition, three concentration-effect curves, each obtained from a different oocyte, were fitted, and the values represent mean ± standard deviation of the estimated parameters.

α4:β2 ratio	EC_{50}	n_H	E_{max}
	μM		*%1 mM ACh*
9:1	58.8 ± 14.7	1.33 ± 0.19	105.9 ± 2.7
1:1	65.6 ± 28.6[c]	1.14 ± 0.07	106.1 ± 2.5
1:1[a]	93.6 ± 14.7[c]	1.36 ± 0.15	105.8 ± 1.7
1:9[b]	1.84 ± 0.09[d]	1.05 ± 0.05	89.3 ± 6.0

[a] Reduced receptor expression level.
[b] Concentration-effect curve of the component more sensitive to ACh only.
[c] No statistical significant difference (*t* test; p = 0.21).
[d] Statistical significant difference (*t* test; p < 0.001) compared with all other groups.

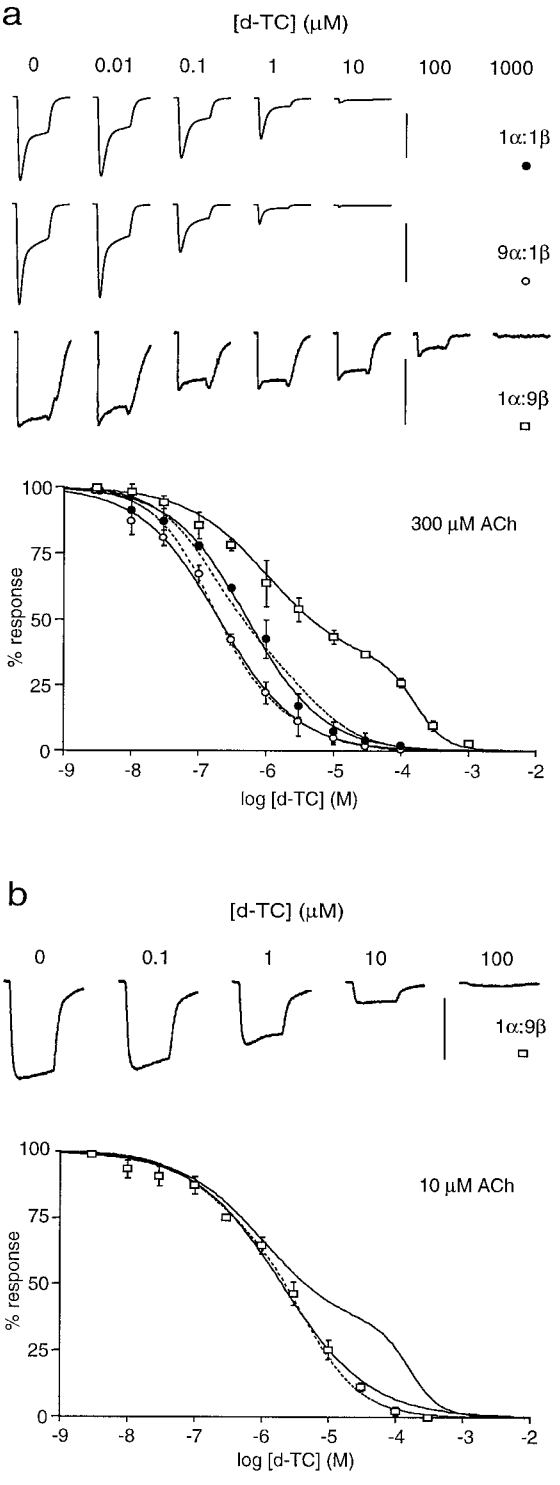

Fig. 3. Concentration-dependent effects of d-TC on $\alpha4\beta2$ nAChRs expressed in *X. laevis* oocytes after injection of cDNAs in the α:β ratios indicated. a, *Top*, inward currents evoked by 10-sec periods of superfusion with external saline containing 300 μM ACh in the presence of d-TC at the concentrations indicated for three oocytes at the 1:1 (●), 9:1 (○), and 1:9 (□) α:β ratios. *Bottom*, dependence of inward current amplitude, normalized to the amplitude of control responses induced by 300 μM ACh, on the concentration of d-TC. Values are mean ± standard deviation obtained from three oocytes. *Drawn lines*, mean of one-component agonist concentration-effect curves fitted to the data obtained for the 1:1 and 9:1 α:β ratios and of two-component concentration-effect curves fitted to the data obtained for the 1:9 α:β ratio to account for a second component of inhibition. The estimated parameters of the fitted curves are presented in Table 2. *Calibrations bars*, 2 μA (1:1), 500 nA (9:1), and 100 nA (1:9). b, Inhibition of inward currents evoked by 10-sec periods of superfusion with external saline containing 10 μM ACh in the presence of d-TC at the concentrations indicated. The low concentration of ACh selectively activates the more-sensitive $\alpha4\beta2$ nAChRs expressed at the 1:9 α:β ratio (see Fig. 2B). *Calibration bar*, 50 nA. *Bottom*, concentration-dependent inhibition of inward current amplitude by d-TC (□), which is fitted by a monophasic inhibition curve (*drawn line*). The biphasic inhibition curve obtained for the inhibition of 300 μM ACh-induced inward current is drawn for comparison. *Dashed inhibition curves* (A and B), results of fitting a model assuming two sites for the inhibition by d-TC contributing differentially to the curves obtained at the different α:β ratios (see Discussion).

Additional experiments were performed to investigate the relation between the two components of inhibition by d-TC (Fig. 3A) and the two components of ACh sensitivity (Fig. 2B) for the 1:9 α:β ratio. Inward currents were evoked by superfusion with 10 μM ACh to selectively activate the more sensitive nAChRs. The data on the inhibition of 10 μM ACh-induced inward current by d-TC are well fitted by a one-component concentration-effect curve (Fig. 3B) with an IC_{50} value (see Table 2) that cannot be distinguished from that of the more-sensitive component of inhibition of 300 μM ACh-evoked responses (t test; $p = 0.11$). Comparison of the inhibition curves of d-TC obtained with 10 and 300 μM ACh (Fig. 3B) shows that at the 1:9 α:β ratio, two subtypes of nAChRs are expressed: one subtype more sensitive to ACh and one less sensitive to d-TC than the receptors expressed at the other α:β ratios, and a second subtype with low sensitivity to ACh and very low sensitivity to d-TC. The IC_{50} of d-TC shifts toward higher concentrations with decreasing α:β ratio (ANOVA; p values < 0.001), and the IC_{50} values of d-TC obtained at the different α:β ratios differ statistically (t test; p values < 0.01; Table 2).

To investigate the mechanism of inhibition of the component of nAChR-mediated ion current with a very low sensitivity to d-TC observed at the 1:9 α:β ratio, oocytes were continuously superfused with 30 μM d-TC to eliminate the more-sensitive component (see Fig. 3A). Inward currents evoked by superfusion with 100 μM ACh in the presence of 30 μM d-TC, which represent the less-sensitive component, and after preexposure to 330 μM d-TC for 4 min were recorded to establish low affinity inhibition. Inward currents evoked at a holding potential of −60 mV were reduced by 81.7 ± 1.6% (three oocytes) by increasing the concentration of d-TC from 30 to 330 μM (Fig. 4A). In the same oocytes, low affinity inhibition at a holding potential of −100 mV (Fig. 4B) amounted to 86.9 ± 2.4%. The small difference is statistically significant (t test; $p < 0.05$), indicating some voltage dependence of the inhibitory effect. Inward currents evoked by coapplication of 100 μM ACh and 330 μM d-TC show a reduction in the peak amplitude and a rapid further onset of inhibition by d-TC during the response (Fig. 4C). At the steady level of inhibition, which was achieved within a few seconds, the amount of reduction of the inward current is the same as that obtained with preexposure to d-TC. The apparent absence of kinetic effects after preexposure to d-TC (Fig. 4, A and B) and the absence of a pronounced tail current on removal of the high concentration of d-TC (Fig. 4C) indicate that ion channel opening is not required for the inhibitory effect. Together with the weak voltage dependence of inhibition, these results indicate that even at high concentrations, d-TC does not cause significant ion channel block.

Effects of nAChR expression level on agonist and antagonist sensitivities. Because it cannot be excluded that nAChR expression level by itself affects agonist and antagonist sensitivity, experiments were performed on oocytes injected with diluted 1:1 α:β cDNA solution at constant injection volume. In oocytes injected with a 10-fold diluted cDNA solution, superfusion with 1 mM ACh did not evoke detectable (>5 nA) inward currents (10 oocytes). This indicates that nAChR expression is greatly reduced, consistent with previous results on the expression level of chick $\alpha4\beta2$ nAChRs in oocytes (Bertrand *et al.*, 1991). After the injection with a 4-fold diluted cDNA solution, ACh-induced ion currents were evoked, which were smaller than those obtained before but had a similar shape (Fig. 5A). The inward current decay at the end of ACh application amounted to 48 ± 15% (five oocytes) of the peak current. This cannot be distinguished from the degree of decay at the higher expression level (*t* test; $p = 0.24$) but differs from the degree of inward current decay obtained for the 1:9 α:β ratio ($p < 0.01$). Agonist and antagonist sensitivities were determined from six oocytes with a maximal peak inward current amplitude of 398 ± 82 nA (i.e., in the same range as with the 1:9 and 9:1 α:β ratios). The results obtained with ACh at concentrations of ≤1 mM from oocytes with high and low level nAChR expression at the 1:1 α:β ratio are not identical (two-way ANOVA; $F_{1,28} = 7.556$, $p = 0.01$). Although the fitted concentration-effect curve of ACh (Fig. 5A, Table 1) shows a small shift toward higher concentrations, the EC_{50} and n_H values cannot be distinguished from those obtained for the higher expression level (*t* test; $p > 0.08$). The concentration-effect curve of d-TC at the low expression level (Fig. 5B, Table 2) cannot be distinguished statistically from that obtained with the high expression level at the 1:1 α:β ratio (two-way ANOVA; $F_{1,20} = 2.290$, $p = 0.15$). However, this curve differs from the inhibition curves obtained for the 9:1 and 1:9 α:β ratios (two-way ANOVA; $p < 0.001$). Further statistical analysis showed that the expression level does not influence the IC_{50} value of d-TC (*t*-test; $p = 0.33$) and that regardless of expression level, distinct IC_{50} values are obtained for the different subunit ratios (*t* test; *p* values < 0.01). From the combined results, it is concluded that reducing the nAChR expression level causes only a small decrease in ACh sensitivity, which is opposite the 30-fold increase in sensitivity observed at the 1:9 α:β ratio.

TABLE 2

Inhibitory effects of d-TC on $\alpha4\beta2$ nAChRs expressed in *Xenopus* oocytes injected with cDNAs encoding α and β subunits in the ratios indicated

Responses were evoked by superfusion with 300 μM ACh. For each experimental condition, three concentration-effect curves, each obtained from a different oocyte, were fitted, and the values represent mean ± standard deviation of the estimated parameters.

$\alpha4$:$\beta2$ ratio	IC_{50}	n_H	E_{max}
	μM		% of control
9:1	0.20 ± 0.04[d]	0.75 ± 0.02	100
1:1	0.53 ± 0.09[de]	0.77 ± 0.13	100
1:1[a]	0.64 ± 0.15[e]	0.71 ± 0.04	100
1:9[b]	1.08 ± 0.75[f]	0.71 ± 0.17	67.6 ± 8.2
	163 ± 37[d]	1.98 ± 0.93	32.4 ± 8.2
1:9[c]	2.04 ± 0.29[df]	0.67 ± 0.03	100

[a] Reduced receptor expression level.
[b] Two-component concentration-effect curve.
[c] Responses evoked by superfusion with 10 μM ACh.
[d] Statistical significant difference (*t* test; $p < 0.01$) between all groups indicated. No statistical significant difference (*t* test; [e] $p = 0.33$, [f] $p = 0.11$).

Discussion

Differences in agonist and antagonist sensitivities of receptors expressed in oocytes after injection of cDNAs coding for the $\alpha4$ and $\beta2$ subunits at 1:9, 1:1, and 9:1 ratios demonstrate heterogeneity of $\alpha4\beta2$ nAChRs. The results show that combinations of $\alpha4$ and $\beta2$ subunits form four pharmacologically distinct subtypes of heteromeric nAChRs. Two subtypes of nAChRs, which are distinguished for the 1:1 and 9:1 α:β ratios, have similar low sensitivities to ACh ($EC_{50} \approx 60$ μM) but distinct sensitivities to d-TC ($IC_{50} = 0.20$ and 0.53 μM, respectively). Two additional, distinct subtypes of nAChRs are formed at the 1:9 α:β ratio: one subtype with markedly enhanced sensitivity to ACh ($EC_{50} = 1.8$ μM) and decreased sensitivity to d-TC ($IC_{50} = 2.04$ μM), and a second subtype with low sensitivity to ACh and very low sensitivity to d-TC ($IC_{50} = 163$ μM). Heterogeneity of neuronal nAChRs has been suggested before from the observation that the occurrence of distinct single-channel conductances in oocytes expressing neuronal-type nAChRs depends on α:β ratio (Papke *et al.*, 1989).

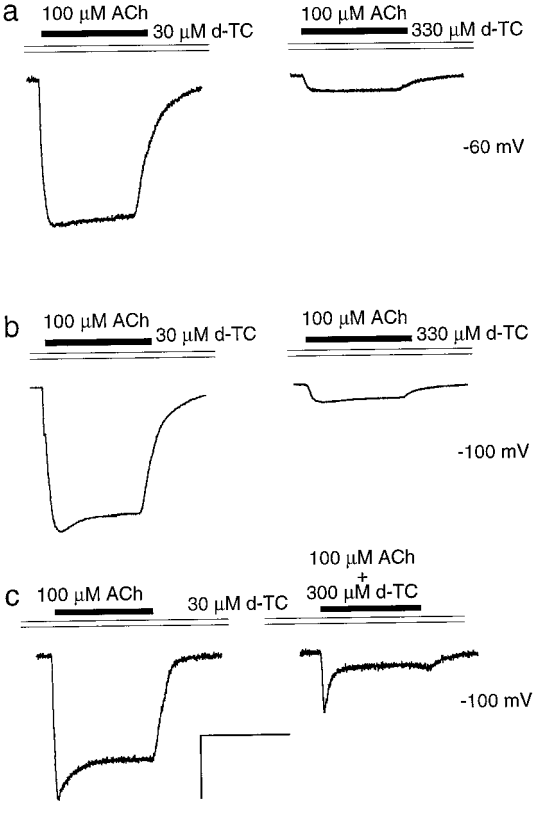

Fig. 4. Ion currents with very low sensitivity to d-TC in oocytes injected with $\alpha4$ and $\beta2$ cDNAs at the 1:9 α:β ratio and the inhibitory effect of a high concentration of d-TC. Oocytes were superfused continuously with 30 μM d-TC to inhibit the d-TC-sensitive component of ACh-induced ion current (see Fig. 3A). a, Inward currents evoked with 100 μM ACh before and 4 min after raising the d-TC concentration to 330 μM at the holding potential of −60 mV. b, Inward currents from the same oocyte demonstrating the inhibitory effect of d-TC at the holding potential of −100 mV. c, Inhibitory effect of coapplication of 100 μM ACh and 330 μM d-TC illustrating a reduced peak inward current amplitude and accelerated inward current decay. *Horizontal calibration bar*, 10 sec. *Vertical calibration bar*, 100 nA (A and C) and 200 nA (B).

The effects of varying α:β ratio on the properties of nAChRs were investigated in oocytes injected with approximately equal total amounts of cDNA (2.5–2.8 ng/oocyte). The reduced response amplitudes at the 1:9 and 9:1 ratios indicate that the availability of α and β subunits limits functional receptor expression at these cDNA ratios (Fig. 1). A comparison of the properties of nAChRs expressed at a reduced level for the 1:1 α:β ratio (Fig. 5) with those of nAChRs expressed at the 1:9 and 9:1 ratios (Figs. 2, 3) demonstrates that the 30-fold difference in sensitivity to ACh, the shift in sensitivity to d-TC, and the differences in the degree of inward current decay are due to changes in subunit ratio and not to differences in expression level.

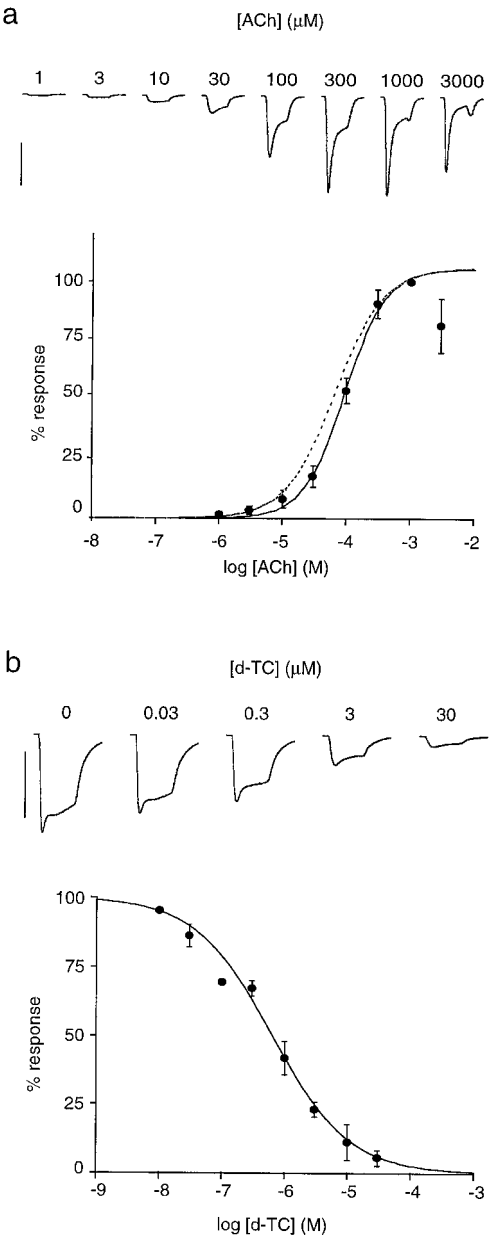

Fig. 5. Agonist and antagonist sensitivities of $\alpha4\beta2$ nAChRs expressed in oocytes injected with 4-fold diluted 1:1 α:β cDNA solution. a, Inward currents evoked by 10-sec periods of superfusion with external saline containing ACh at the concentrations indicated (*calibration bar*, 200 nA). *Bottom*, mean ± standard deviation of peak inward current amplitudes normalized to that of 1 mM ACh-evoked inward currents from three oocytes. The data were fitted by a one-component concentration-effect curve (*drawn line*). For comparison, the concentration-effect curve obtained for $\alpha4\beta2$ nAChRs at the higher expression level with the 1:1 α:β ratio (Fig. 2A) is drawn (*dashed line*). Data obtained at 1 mM ACh, which induced ion channel block, are not included in the fit. b, Inhibition of 300 μM ACh-induced inward current by d-TC at the concentrations indicated (*calibration bar*, 500 nA). *Bottom*, mean ± standard deviation (three oocytes) of peak inward current amplitudes normalized to that of 300 μM ACh-evoked control responses. *The two data points without error bars*, from one oocyte. The data were fitted by a one-component concentration-effect curve (*drawn line*). The estimated parameters of the curves fitted to the data in A and B are presented in Tables 1 and 2, respectively.

The properties of ligand-gated ion channels depend on subunit composition. Combining $\alpha4$ and $\beta2$ subunits into a pentameric nAChR protein theoretically can yield eight distinct subtypes of the $\alpha4\beta2$ nAChR. The two homopentameric $\alpha4$ and $\beta2$ nAChRs are not expressed or are not functional. Six heteropentameric subunit assemblies remain: four α:β subunit stoichiometries (1:4, 2:3, 3:2, and 4:1) and two alternative subunit arrangements for the 2:3 and the 3:2 stoichiometries (Fig. 6). Of these six, at least four have been demonstrated to form pharmacologically distinct, functional nAChRs. This implies that functional $\alpha4\beta2$ nAChRs are formed with other than the 2:3 α:β subunit stoichiometry.

Functional heteropentameric neuronal nAChRs presumably contain two binding sites for ACh located at the $\alpha\beta$ interfaces (Luetje and Patrick, 1991; Bertrand and Changeux, 1995). However, only two of all possible subunit assemblies contain two $\alpha\beta$ interfaces (Fig. 6). The conclusion that four distinct types of $\alpha4\beta2$ nAChRs are formed implies that agonist binding at one or more of the $\beta\alpha$, $\beta\beta$, or $\alpha\alpha$ subunit interfaces may be involved in ion channel activation or that binding of a single agonist molecule is sufficient to activate $\alpha4\beta2$ nAChRs. The latter would be consistent with the results because the slopes of the concentration-effect curves of ACh all are close to 1 (Table 1). Shallow slopes of the concentration-effect curve of ACh on $\alpha4\beta2$ nAChRs generally are reported: in oocyte studies, 0.81 for rat $\alpha4\beta2$ (Stafford *et al.*, 1994), 1.5 for chick $\alpha4\beta2$ (Bertrand *et al.*, 1990), and 1.02 for human $\alpha4\beta2$ (Chavez-Noriega *et al.*, 1997), and in human embryonic kidney 293 cells, 1.2 for human $\alpha4\beta2$ (Buisson and Bertrand, 1998). In $\alpha7$ nAChRs, $\alpha\alpha$ interfaces contribute to ligand binding. This homopentameric nAChR seems to contain five binding sites for the competitive antagonist methyllycaconitine (Palma *et al.*, 1996). The $\alpha7$ subunit contains the principal component (loops A–C) as well as the highly conserved residue Trp54, which constitutes part of a complementary component of the proposed agonist binding site. These two components of the agonist binding site in $\alpha7$ are thought to be equivalent to those contained by the muscle-type $\alpha1$ and the γ and δ nAChR subunits, respectively. The $\alpha4$ subunit contains the principal component of the agonist binding site as well as a tryptophan residue homologous to

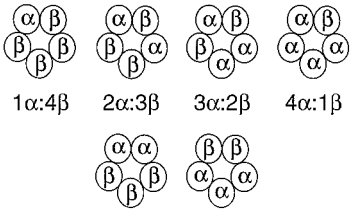

Fig. 6. Schematic representation of the six possible arrangements of α and β subunits within heteropentameric nAChRs. Note the two alternative subunit arrangements for the 2:3 and 3:2 α:β subunit stoichiometries.

Trp54 in α7. The β2 subunit contains the complementary component of the agonist binding site as well as loops A and B of the principal component (Corringer *et al*., 1995). The homology among α4, β2, and α7 suggests that $\alpha\alpha$, $\beta\alpha$, or $\beta\beta$ subunit interfaces also might form functional agonist or antagonist binding sites. The shift in agonist sensitivity seems to be specific for the $\alpha4\beta2$ nAChRs because it is not observed when $\alpha3\beta2$ and $\alpha4\beta4$ nAChRs are expressed at 1:1 and 1:9 α:β cDNA ratios (Luetje and Patrick, 1991). This indicates that neither $\alpha\alpha$ nor $\beta\beta$ subunit interfaces are directly involved in the change in sensitivity to ACh.

The results show that the inhibitory effects of d-TC on $\alpha4\beta2$ nAChRs are not due to ion channel block. Low concentrations of d-TC have been shown to inhibit neuronal nAChRs by a competitive interaction before (Bertrand *et al*., 1990), but the exact nature of the inhibitory effect of the very high concentrations of d-TC on nAChRs at the 1:9 α:β ratio remains to be investigated. However, the four distinct IC_{50} values for d-TC do not necessarily imply that $\alpha4\beta2$ nAChRs contain four distinct binding sites for d-TC. Apart from the component with very low sensitivity, the effects of d-TC consist of monophasic inhibition curves with shallow slopes, which gradually shift to higher concentrations with decreasing α:β ratio (Fig. 3; Table 2). This indicates that high and low affinity sites differentially contribute to the inhibitory effect of d-TC and cause shift of the IC_{50}. Three two-component inhibition curves of d-TC were simultaneously fitted to the three sets of data obtained for the 9:1, 1:1, and 1:9 (10 μM ACh) α:β ratios. Hill coefficients were set to 1, and the IC_{50} values of d-TC and the relative proportions of the two effects of d-TC were estimated. This yielded IC_{50} values of 0.16 and 4.3 μM d-TC, regardless of α:β ratio. The estimated proportions of the more- and less-sensitive components changed with α:β ratio. The size of the more sensitive component decreased from 88% at the 9:1 α:β ratio to 62% and further to 26% at the 1:1 and 1:9 α:β ratios, respectively. The curves fitted according to the two-component inhibition model (Fig. 3) demonstrate that for $\alpha4\beta2$ nAChRs, at least two sites with an estimated 27-fold difference in sensitivity to d-TC are required to account for the inhibitory effects observed. This is in the same order of magnitude as the 15- and 27-fold differences in sensitivity of $\alpha1\beta1\gamma$ and $\alpha1\beta1\delta$ muscle-type nAChRs expressed in fibroblasts and human embryonic kidney 293 cells to d-TC and dimethyl-d-TC, respectively (Blount and Merlie, 1989; Sine, 1993). The shift in the inhibition curve of d-TC can be accounted for by assuming a minimum of two distinct sites for d-TC. The differential contribution of these sites to the inhibitory effect at different α:β ratios suggests that they are located on distinct subtypes of $\alpha4\beta2$ nAChRs. The possibility that the high and low affinity components reflect effects of d-TC on a single population of receptors is highly unlikely. If the two sites would be present on the same nAChR, only the inhibition caused by the binding of d-TC to the high affinity site would have been detected. Some receptors seem to lack both sites because they are affected by d-TC at very high concentrations only.

The results with d-TC indicate that two subtypes of $\alpha4\beta2$ nAChRs may be distinguished in oocytes injected with cDNAs at the 1:1 α:β ratio. In oocytes injected with cRNAs or cDNAs encoding chick α4 and β2 subunits at a 1:1 ratio, nAChRs seem to have a 2:3 α:β stoichiometry (Anand *et al*., 1991; Cooper *et al*., 1991). The current and the previous results are compatible when two subunit arrangements, which are possible for the 2:3 α:β stoichiometry (Fig. 6), are formed and have distinct sensitivities to d-TC. The diverging results on the number of conductance levels of single ion channels formed by $\alpha4\beta2$ nAChRs at the 1:1 α:β ratio provide no conclusive evidence on $\alpha4\beta2$ nAChR heterogeneity (Papke *et al*., 1989; Cooper *et al*., 1991; Charnet *et al*., 1992; Kuryatov *et al*., 1997). Single-channel properties of $\alpha4\beta2$ nAChRs at other than the 1:1 α:β ratio have not been reported. Whether the arrangement of subunits within a receptor affects single-channel properties remains unknown. The current results demonstrate that changing the relative abundance of subunits expressed by changing the cDNA ratio leads to alternative subunit assemblies with sensitivities to ACh and d-TC distinct from those obtained for nAChRs at the 1:1 α:β ratio.

The ratios of subunit cDNAs used in the current study for the expression of distinct subtypes of $\alpha4\beta2$ nAChRs in oocytes are in the same order of magnitude as those found in brain. The ratio of α4:β2 mRNA levels in various regions of rat brain ranges between 1:1 and 1:15 (Liu *et al*., 1996). For α-amino-3-hydroxy-5-methyl-4-isoxazolepropionic acid-type glutamate receptors, it has been shown that the number of glutamic acid type 2 receptor subunits incorporated depends on the relative abundance of the glutamic acid type 2 receptor subunit expressed in oocytes as well as in rat hippocampal interneurons. The resulting differences in subunit stoichiometry of native and heterologously expressed α-amino-3-hydroxy-5-methyl-4-isoxazolepropionic acid receptors are associated with changes in channel function (Washburn *et al*., 1997). Although it was assumed previously that nAChRs have a fixed subunit stoichiometry, the current results show that $\alpha4\beta2$ nAChR subunit stoichiometry also can be changed by altering the relative abundance of α and β subunits. Thus, changing the subunit stoichiometry of receptors by selective up- or down-regulation of the expression level of specific subunits seems to be a more general mechanism to tune the properties of ligand-gated ion channels. The current observation that agonist and antagonist sensitivities depend on subunit stoichiometry provides a rational basis for the existence of heteromeric neuronal nAChRs.

Acknowledgments

We thank Dr. Jim Patrick (Baylor College of Medicine, Houston, TX) for donating the cDNA clones of nAChR subunits, Kees Koster (Hubrecht Laboratory, Utrecht, The Netherlands) for supplying *X. laevis* oocytes, John Rowaan for taking care of the frogs in our laboratory, and Ing. Aart de Groot for excellent technical assistance.

References

Anand R, Conroy WG, Schoepfer R, Whiting P, and Lindstrom J (1991) Neuronal nicotinic acetylcholine receptors expressed in *Xenopus* oocytes have a pentameric quaternary structure. *J Biol Chem* **266:**11192–11198.

Bertrand D, Ballivet M, and Rungger D (1990) Activation and blocking of neuronal nicotinic acetylcholine receptor reconstituted in *Xenopus* oocytes. *Proc Natl Acad Sci USA* **87:**1993–1997.

Bertrand D and Changeux JP (1995) Nicotinic receptor: an allosteric protein specialized for intercellular communication. *Semin Neurosci* **7:**75–90.

Bertrand D, Cooper E, Valera S, Rungger D, and Ballivet M (1991) Electrophysiology of neuronal nicotinic acetylcholine receptors expressed in *Xenopus* oocytes following nuclear injection of genes or cDNAs. *Methods Neurosci* **4:**174–193.

Blount P and Merlie JP (1989) Molecular basis of the two nonequivalent ligand binding sites of the muscle nicotinic receptors. *Neuron* **3:**349–357.

Buisson B and Bertrand D (1998) Open-channel blockers at the human $\alpha4\beta2$ neuronal nicotinic acetylcholine receptor. *Mol Pharmacol* **53:**555–563.

Buller AL and White MM (1990) Functional acetylcholine receptors expressed in *Xenopus* oocytes after injection of *Torpedo* β, γ, and δ subunit RNAs are a consequence of endogenous oocyte gene expression. *Mol Pharmacol* **37:**423–428.

Charnet P, Labarca C, Cohen BN, Davidson N, Lester HA, and Pilar G (1992) Pharmacological and kinetic properties of $\alpha 4\beta 2$ neuronal nicotinic acetylcholine receptors expressed in *Xenopus* oocytes. *J Physiol (Lond)* **450:**375–394.

Chavez-Noriega LE, Crona JH, Washburn MS, Urrutia A, Elliott KJ, and Johnson EC (1997) Pharmacological characterization of recombinant human neuronal nicotinic acetylcholine receptors h$\alpha 2\beta 2$, h$\alpha 2\beta 4$, h$\alpha 3\beta 2$, h$\alpha 3\beta 4$, h$\alpha 4\beta 2$, h$\alpha 4\beta 4$ and h$\alpha 7$ expressed in *Xenopus* oocytes. *J Pharmacol Exp Ther* **280:**346–356.

Colquhoun D, Dryer F, and Sheridan RE (1979) The actions of tubocurarine at the frog neuromuscular junction. *J Physiol (Lond)* **293:**247–284.

Colquhoun D and Ogden DC (1988) Activation of ion channels in the frog end-plate by high concentrations of acetylcholine. *J Physiol (Lond)* **395:**131–159.

Cooper E, Couturier S, and Ballivet M (1991) Pentameric structure and subunit stoichiometry of a neuronal nicotinic acetylcholine receptor. *Nature (Lond)* **350:** 235–238.

Corringer PJ, Galzi JL, Eiselé JL, Bertrand S, Changeux JP, and Bertrand D (1995) Identification of a new component of the agonist binding site of the nicotinic $\alpha 7$ homooligomeric receptor. *J Biol Chem* **270:**11749–11752.

Flores CM, Rogers SW, Pabreza LA, Wolfe BB, and Kellar KJ (1992) A subtype of nicotinic cholinergic receptor in rat brain is composed of $\alpha 4$ and $\beta 2$ subunits and is up-regulated by chronic nicotine treatment. *Mol Pharmacol* **41:**31–37.

Kuryatov A, Gerzanich V, Nelson M, Olale F, and Lindstrom J (1997) Mutation causing autosomal dominant nocturnal frontal lobe epilepsy alters Ca^{2+} permeability, conductance, and gating of human $\alpha 4\beta 2$ nicotinic acetylcholine receptors. *J Neurosci* **17:**9035–9047.

Liu C, Nordberg A, and Zhang X (1996) Differential co-expression of nicotinic acetylcholine receptor $\alpha 4$ and $\beta 2$ subunit genes in various regions of rat brain. *NeuroReport* **7:**1645–1649.

Luetje CW and Patrick J (1991) Both the α- and β-subunits contribute to the agonist sensitivity of neuronal nicotinic acetylcholine receptors. *J Neurosci* **11:**837–845.

McGehee DS and Role LW (1995) Physiological diversity of nicotinic acetylcholine receptors expressed by vertebrate neurons. *Annu Rev Physiol* **57:**521–546.

Oortgiesen M and Vijverberg HPM (1989) Properties of neuronal type acetylcholine receptors in voltage clamped mouse neuroblastoma cells. *Neuroscience* **31:**169–179.

Palma E, Bertrand S, Binzoni T, and Bertrand D (1996) Neuronal nicotinic $\alpha 7$ receptor expressed in *Xenopus* oocytes presents five putative binding sites for methyllycaconitine. *J Physiol (Lond)* **491:**151–161.

Papke RL, Boulter J, Patrick J, and Heinemann S (1989) Single-channel currents of rat neuronal nicotinic acetylcholine receptors expressed in *Xenopus* oocytes. *Neuron* **3:**589–596.

Papke RL and Heinemann SF (1991) The role of the $\beta 4$ subunit in determining the kinetic properties of rat neuronal nicotinic acetylcholine $\alpha 3$ receptors. *J Physiol (Lond)* **440:**95–112.

Sine SM (1993) Molecular dissection of subunit interfaces in the acetylcholine receptor: identification of residues that determine curare selectivity. *Proc Natl Acad Sci USA* **90:**9436–9440.

Stafford GA, Oswald, RE, and Weiland GA (1994) The β subunit of neuronal nicotinic acetylcholine receptors is a determinant of the affinity for substance P inhibition. *Mol Pharmacol* **45:**758–762.

Wada E, Wada K, Boulter J, Deneris ES, Heinemann S, Patrick J, and Swanson LW (1989) Distribution of $\alpha 2$, $\alpha 3$, $\alpha 4$, and $\beta 2$ neuronal nicotinic receptor subunit mRNAs in the central nervous system: a hybridization histochemical study in the rat. *J Comp Neurol* **284:**314–335.

Washburn MS, Numberger M, Zhang S, and Dingledine R (1997) Differential dependence on GluR2 expression of three characteristic features of AMPA receptors. *J Neurosci* **17:**9393–9406.

Whiting P, Schoepfer R, Lindstrom J, and Priestley T (1990) Structural and pharmacological characterization of the major brain nicotinic acetylcholine receptor subtype stably expressed in mouse fibroblasts. *Mol Pharmacol* **40:**463–472.

Zwart R, Oortgiesen M, and Vijverberg HPM (1995) Differential modulation of $\alpha 3\beta 2$ and $\alpha 3\beta 4$ neuronal nicotinic receptors expressed in *Xenopus* oocytes by flufenamic acid and niflumic acid. *J Neurosci* **15:**2168–2178.

Zwart R and Vijverberg HPM (1997) Potentiation and inhibition of neuronal nicotinic receptors by atropine: competitive and noncompetitive effects. *Mol Pharmacol* **52:**886–895.

Send reprint requests to: Dr. R. Zwart, Research Institute of Toxicology, Utrecht University, P.O. Box 80.176, NL-3508 TD Utrecht, The Netherlands. E-mail: r.zwart@ritox.vet.uu.nl